ORIGINAL ARTICLE

Cancer Science WILEY

Prognostic relevance of tumor-resident memory T cells in metastatic lymph nodes of esophageal squamous cell carcinoma

Seiji Natsuki [ORCID] | **Hiroaki Tanaka** | **Masaki Nishiyama** | **Takuya Mori** [ORCID] | **Sota Deguchi** | **Yuichiro Miki** | **Mami Yoshii** | **Tatsuro Tamura** | **Takahiro Toyokawa** | **Shigeru Lee** | **Kiyoshi Maeda**

Department of Gastroenterological Surgery, Osaka City University Graduate School of Medicine, Osaka, Japan

Correspondence
Hiroaki Tanaka, 1-4-3 Asahi-machi, Abeno-ku, Osaka-shi, Osaka 545-8585, Japan.
Email: hiroakitan@omu.ac.jp

Abstract

Tumor-resident memory T (T_{RM}) cells in primary tumors are reportedly associated with a favorable prognosis in several malignancies. However, the behaviors and functions of T_{RM} cells in regional lymph nodes (LNs) of esophageal cancer remain poorly understood. The aim of this study was to elucidate the effects of T_{RM} cells in regional LNs of esophageal cancer on clinicopathological findings and prognosis. Specimens of esophageal cancer and primary metastatic LNs (recurrent nerve LNs) were obtained from 84 patients who underwent radical esophagectomy between 2011 and 2017. We performed immunohistochemistry to enumerate and analyze T_{RM} cells, and used flow cytometry to investigate the function of T_{RM} cells. T_{RM} cells were observed in both metastatic LNs and primary tumors. T_{RM} cell-rich specimens exhibited reduced lymphatic invasion and LN metastasis and prolonged survival compared with T_{RM} cell-poor specimens. T_{RM} cells in metastatic LNs were more significantly associated with enhanced survival than T_{RM} cells in primary tumors. T_{RM} cells expressed high levels of granzyme B as a cytotoxicity marker. Our results suggested that high T_{RM} cell infiltration in metastatic LNs improves survival even though LN metastasis is commonly associated with poor prognosis. T_{RM} cells possibly contribute to antitumor immunity in regional LNs.

KEYWORDS
antitumor immunity, CD103, esophageal cancer, lymph node metastasis, tissue-resident memory T cell

---

----

1 | INTRODUCTION

Esophageal squamous cell carcinoma (ESCC) is the predominant histological subtype worldwide and known for its very poor prognosis, which is related to high rates of recurrence and lymph node (LN) metastasis.[1] In our opinion, further investigation of antitumor immune response within metastatic LNs may enable us to uncover antitumor immunity of regional LNs, which remains poorly understood. Among regional LNs, the recurrent nerve LNs, which are designated No. 106rec LNs according to the 11th edition of the Japanese Classification of Esophageal Cancer,[2] play a crucial role in ESCC because they exhibit a high rate of metastasis and function as sentinel LNs, which are the first LNs receiving lymphatic drainage from the primary tumor.[3,4] In addition, No. 106rec LNs locate around the important organ, which is the recurrent nerve. Surgical procedures involving extensive LN dissection occasionally cause recurrent nerve palsy, which sometimes results in postoperative aspiration pneumonia as a fatal post-surgical complication. Considering the predicted future increases in the number of elderly patients, unnecessary LN dissection should be avoided. If a strong antitumor immune response could be induced within No. 106rec LNs, dissection might be rendered unnecessary.

CD8$^+$ tumor-infiltrating lymphocytes play an important role in antitumor immunity and are associated with a favorable prognosis in many kinds of tumors, as summarized in several reviews.[5–8] CD8$^+$CD103$^+$ T cells, also referred to as tissue-resident memory T (T_{RM}) cells, are noteworthy in that they are associated with significantly improved survival in some carcinomas.[9–12] T_{RM} cells generally reside in the peripheral tissues, including tumoral lesions, and they never recirculate into the blood.[13] These cells are characterized and defined by expression of the CD103 antigen, also known as integrin αE/β7, which binds to E-cadherin.[14] Although several studies have documented a positive effect of T_{RM} cells in primary lesions on prognosis, the effect of T_{RM} cells in the secondary lymphoid organs remains to be elucidated.

In this study, we targeted T_{RM} cells in No. 106rec LNs to determine whether the antitumor immune response within the tumor-draining LNs of ESCC contributes to prognosis.

2 | MATERIALS AND METHODS

2.1 | Patients and samples

We surveyed our department data, which included 639 patients who underwent radical esophagectomy for thoracic esophageal cancer at Osaka City University (currently Osaka Metropolitan University, Osaka, Japan) between 2011 and 2017 (Figure 1A). The mean follow-up time was 54 months (range, 0–135 months). To examine details regarding No. 106rec LN metastasis, we excluded patients with (i) incomplete data (6 cases), (ii) residual tumors (R1 or R2; 43 cases), (iii) salvage surgery (60 cases), (iv) neoadjuvant chemoradiotherapy (23 cases), (v) post-endoscopic submucosal resection (39 cases), or (vi) no SCC histologically (six cases). A total of 462 patients were finally included in the investigation of the clinical significance and T_{RM} cells of No. 106rec LNs. Exclusion criteria were defined to evaluate primary lesions over the same period. A total of 84 of these patients presented with No. 106rec LN metastasis and were, therefore, included in the study.

Metastatic LNs (No. 106rec) and primary tumor samples were obtained from the 84 included patients. The mean patient age was 65.8 years (range, 48–82 years), and the group included 73 (86.9%) men and 11 (13.1%) women. A total of 66 of the 84 (78.6%) patients received neoadjuvant chemotherapy (NAC). Indications for preoperative chemotherapy and details of the regimens were in accordance with relevant esophageal cancer treatment guidelines. The preoperative regimen was two cycles of 5-FU+cisplatin (FP), 5-FU+nedaplatin (FGP), or docetaxel+cisplatin +5-FU (DCF). FP consisted of a 4-week cycle of fluorouracil at a dose of 800 mg/m^2 of body surface area on days 1 to 5 and cisplatin at a dose of 80 mg per square meter on day 1. FGP consisted of a 4-week cycle of fluorouracil at a dose of 800 mg/m^2 on days 1 to 5 and nedaplatin at a dose of 90 mg per square meter on day 1. DCF consisted of a 4-week cycle of fluorouracil at a dose of 800 mg/m^2 on days 1 to 5, cisplatin at a dose of 80 mg/m^2 on day 1, and docetaxel at a dose of 30 mg/m^2 on days 1 and 15.

The chemotherapy dose was reduced as needed in accordance with the patient's condition and adverse events. The mean follow-up time was 30.0 months (range, 2–89 months). Based on the Japanese Classification,[2] the tumor locations were defined as upper thoracic esophagus (Ut)/middle thoracic esophagus (Mt)/lower thoracic esophagus (Lt), and histological type was indicated as differentiated type (well differentiated/moderately differentiated)/undifferentiated type (poorly differentiated). All pathological stages were recorded according to the 8th UICC TNM Classification.[15]

This study was carried out in accordance with the Declaration of Helsinki and approved by the Osaka City University Ethics Committee. Written informed consent was obtained from all patients before enrollment.

2.2 | Efficacy index

The role of No. 106rec LNs in ESCC was examined based on the efficacy index (EI), defined as the effect on survival time of the dissection of each LN type.[3] The EI was calculated as follows: frequency (%) of metastasis to each LN × 5-year survival rate (%) of patients with metastasis to that LN ÷ 100.[3,16]

2.3 | Immunohistochemistry

Metastatic LNs and primary tumors of human specimens from patients with ESCC were embedded in paraffin blocks, cut into 4-μm-thick sections, and fixed with 10% formalin at room temperature for 6 to 48 h. After incubation at 60°C for 10 min, the sections
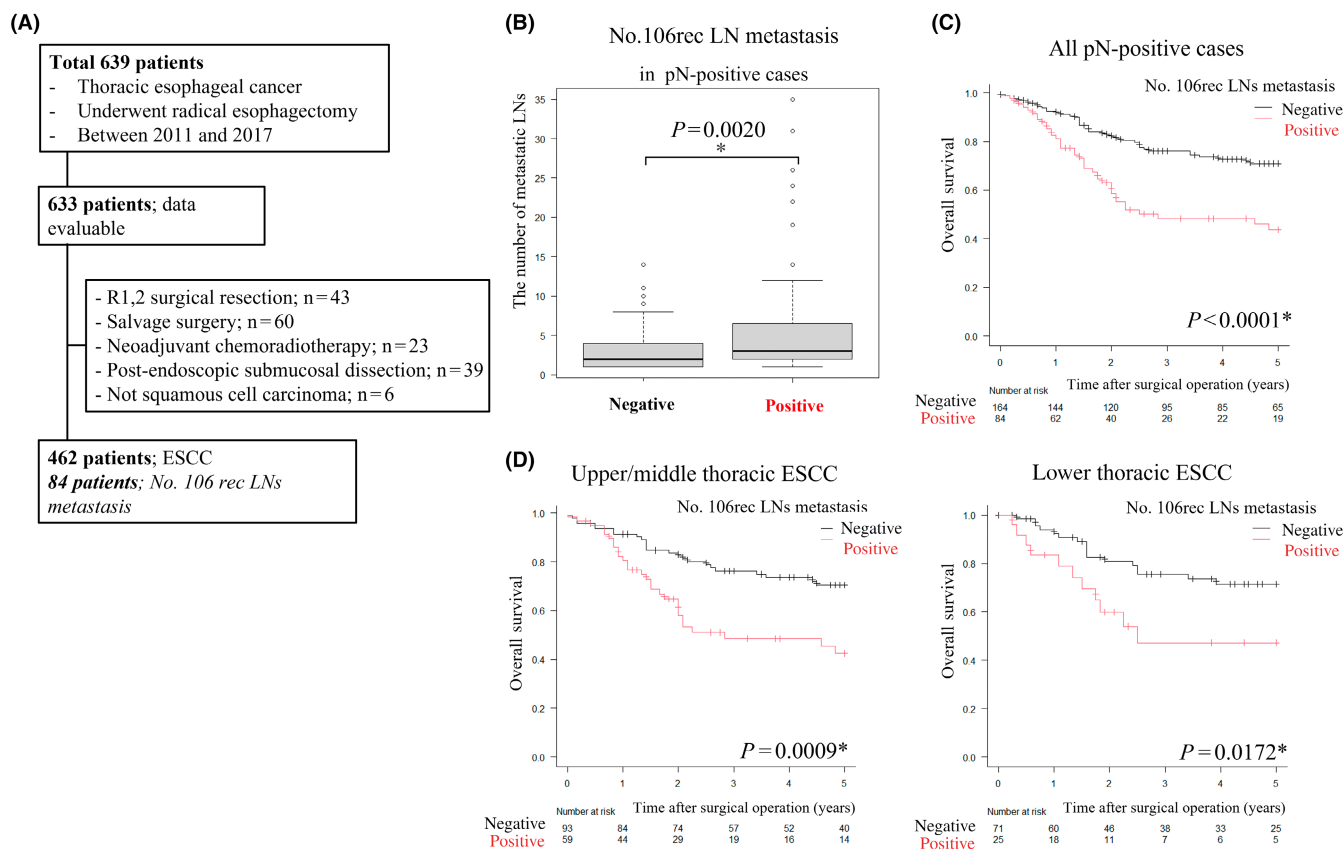
FIGURE 1 (A) Patient disposition chart. (B) Box plot. Comparison of the number of metastatic lymph nodes (LNs) between No. 106rec positive and negative in pN-positive cases. *$p < 0.05$, statistically significant. (C, D) Comparison of overall survival (OS) based on No. 106rec LN metastasis in pN-positive cases using Kaplan–Meier plots and the log-rank test. *$p < 0.05$, statistically significant. (C) All pN-positive cases. (D) Ut/Mt or Lt cases.

were deparaffinized with xylene and rehydrated twice in a stepwise ethanol series (70%, 80%, 90%, and 100%) for 3 min each. Endogenous peroxidase activity was quenched by treatment in 3% hydrogen peroxide with absolute methanol at room temperature for 15 min. After washing in PBS, the sections were autoclaved at 121°C for 10 min for antigen retrieval using Target Retrieval Solution (100× citrate buffer [pH 6.0]; Dako, Agilent Technologies). Nonspecific binding was blocked using nonspecific staining blocking reagent (pre-diluted; Nichirei Biosciences). The sections were then reacted with the primary antibody overnight at 4°C and subsequently incubated with secondary antibody and streptavidin–horseradish peroxidase (pre-diluted; Nichirei Biosciences) for 10 and 5 min each at room temperature. After washing in PBS, the sections were visualized by treatment with 3,3′-diamino-benzidine for 5 min and then counterstained with hematoxylin for 30 s at room temperature before mounting. The primary antibodies used in the study were as follows: rabbit monoclonal anti-CD103 (clone: EPR4166(2); cat. no. ab1292202; 1/1000; Abcam), mouse monoclonal anti-CD8 (clone: C8/144B; cat. no. M7103; 1/250; Dako), rabbit monoclonal anti-CD4 (clone: EPR6855; cat. no. ab133616; 1/250; Abcam), mouse monoclonal anti-E-cadherin (clone: NCH-38; cat. no. M3612; 1/200; Dako), mouse monoclonal anti-HLA-class I (clone: HC10; cat. no. MUB2037P; 1/200; Nordic-MUbio), and mouse monoclonal

anti-HLA-class II (clone: CR3/43; cat. no. sc-53,302; 1/200; Santa Cruz Biotechnology).

2.4 | Evaluation of immunohistochemical staining

Metastatic LNs and primary tumor sections stained with anti-CD103 antibody were scanned at ×400 magnification. The five most-representative high-power fields including CD103+ cells were randomly selected regardless of tumor or metastatic location. We calculated the average number of CD103+ cells in five fields. All microscopic images were imported from the DP-73 digital photo filing system (Olympus). The cut-off value was determined from a time-dependent receiver operating characteristic (ROC) curve of five-year postoperative survival as the stated variable. The ROC curve is shown in Figure S1. We divided the patients into two groups according to this value.

2.5 | Immunofluorescence double staining

Human specimens of metastatic LNs in paraffin-embedded blocks were cut into 4-μm-thick sections. After heat-mediated antigen

Non-metastatic LN

Metastatic LN
CD103 low

CD103 high

Primary tumor
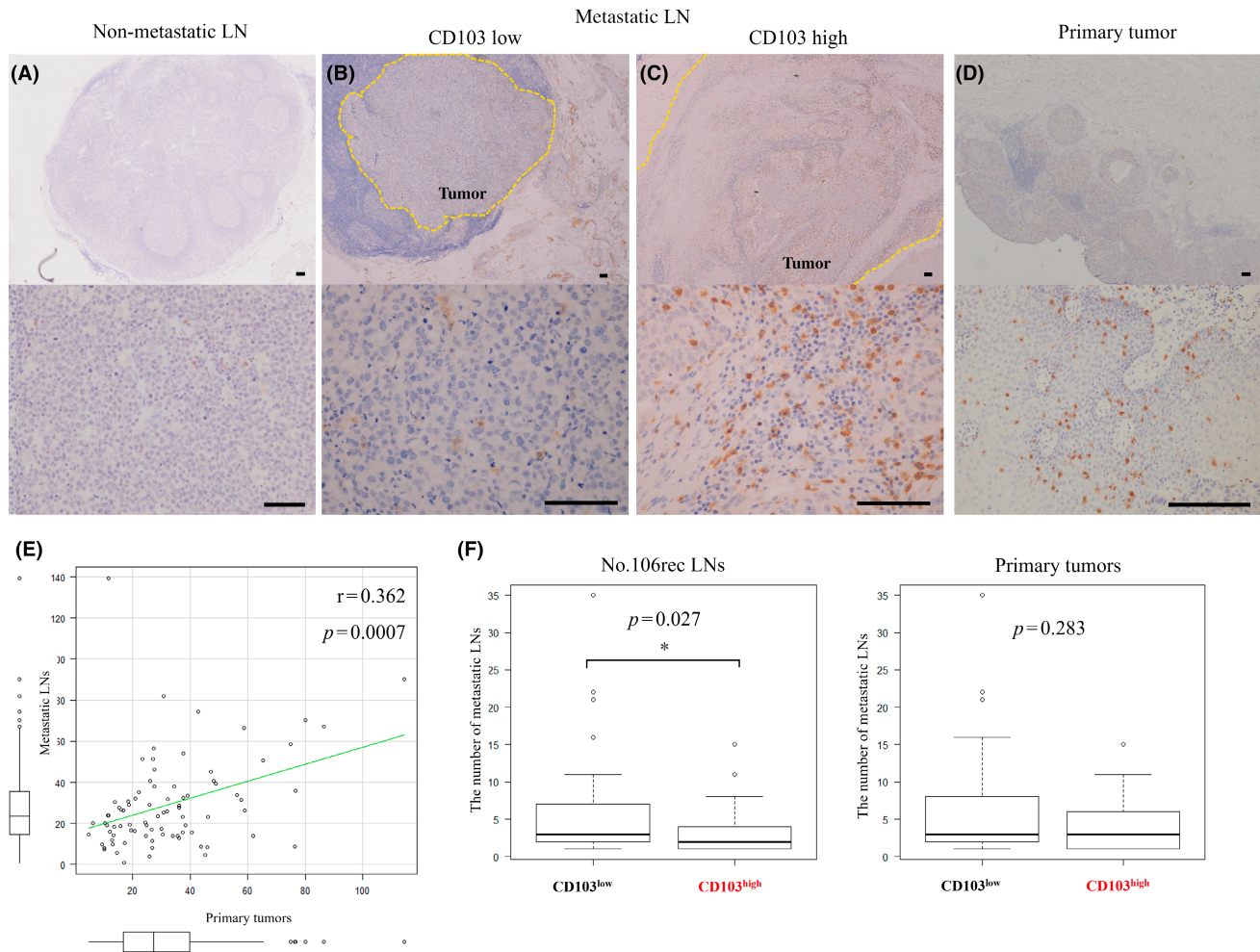
FIGURE 2 (A–D) Representative images of immunohistochemical analysis using an anti-CD103 antibody. Scale bar, 100 μm. (A) Normal lymph nodes (LNs). (B) CD103+ cells poorly infiltrating metastatic LNs. (C) CD103+ cells highly infiltrating metastatic LNs. (D) Primary tumor. (E) We compared CD103 expression between metastatic LNs and primary lesions using Spearman's rank correlation coefficient. (F) Comparison of CD103high and CD103low groups in terms of the number of metastatic LNs among all LNs or primary tumors using the Mann–Whitney U test. *$p < 0.05$, statistically significant.

retrieval and immunohistochemical analysis, nonspecific binding was blocked using nonspecific staining blocking reagent (Dako). The sections were incubated with rabbit monoclonal anti-CD103 antibody (clone: EPR4166(2); 1/1000: Abcam), mouse monoclonal anti-CD8 antibody (clone: C8/144B; 1/250: Dako), mouse monoclonal anti-granzyme B antibody (cat. no. sc-8022; 1/100; Santa Cruz Biotechnology), and mouse monoclonal anti-CD11c antibody (cat. no. ab215858; 1/100; Abcam) at 4°C overnight. The sections were subsequently incubated with Alexa Fluor 488-labeled goat polyclonal anti-rabbit IgG antibody (cat. no. ab150113; 1/1000: Abcam) and Alexa Fluor 647-labeled goat polyclonal anti-rabbit IgG antibody (cat. no. ab150079; 1/1000: Abcam) for 1 h at room temperature. Prolong Gold antifade reagent with DAPI (cat. no. P36935; Invitrogen/Thermo Fisher Scientific) was then added to the sections and covered with glass coverslips. Digital images were taken using an all-in-one fluorescence microscope (BZ-8000: Keyence).

2.6 | Flow cytometry

Flow cytometry was performed to analyze the surface and intracellular markers of T_{RM} cells in single-cell suspensions of LNs obtained from freshly resected tumors from esophageal cancer patients. Approximately 1 cm^3 of tissue was sampled partially from suspected metastatic LNs before surgery; the samples were confirmed as metastatic pathologically ($n = 8$). The tissues were first minced and digested with type I collagenase (1 mg/mL) in RPMI-1640 medium (FUJIFILM Wako Pure Chemical) at 37°C for 30 min. Subsequently, the cell suspension was filtered through a 70-μm nylon mesh (BD Falcon; BD Biosciences).

To assess the production of intracellular cytokines by T cells, CD8+ T cells were stimulated using a T Cell Activation/Expansion Kit, Human (Mitenyi Biotec) according to the manufacturer's instructions. After incubation for 48 h at 37°C in a humidified incubator, the cells were collected and washed with PBS, saturated with BD

TABLE 1 Association between clinicopathological features and infiltration of CD103$^+$ T cell into metastatic lymph nodes (LNs).

		CD103+ cells		
	n	Low (*n* = 51)	High (*n* = 33)	*p*-Value*
Age				
<60year	63	36	27	0.307
>60year	21	15	6	
Sex				
Female	11	8	3	0.515
Male	73	43	30	
Location				
Ut	20	11	9	0.844
Mt	39	24	15	
Lt	25	16	9	
Histological type				
Well	8	5	3	0.529
Moderate	46	28	18	
Poor	22	15	7	
Unknown	8	3	5	
Neoadjuvant chemotherapy				
+	66	40	26	1
−	18	11	7	
pT[a]				
T1	23	12	11	0.0648
T2	19	8	11	
T3	40	29	11	
T4	2	2	0	
pN[a]				
N1	36	18	18	0.117
N2	29	18	11	
N3	19	15	4	
pStage[a]				
Stage II	17	8	9	0.266
Stage III	51	31	20	
Stage IV	16	12	4	
pN-JC[b]				
N1	29	13	15	0.235
N2	43	29	14	
N3	11	8	3	
N4	2	1	1	
Lymphatic invasion				
+	58	41	17	0.0077*
−	26	10	16	
Venous invasion				
+	19	12	7	1
−	65	39	26	

*Fisher's exact probablity test; $p < 0.05$, statistically significant.
[a]TNM Classification of Esophageal squamous cell carcinoma, 8th ed.
[b]Japanese Classificasion of Esophageal Cancer, 11th ed.

Fetal Bovine Serum Stain Buffer (BD Biosciences) and then incubated at 4°C for 30min with the following antibodies against surface markers: FITC-labeled anti-CD3 (clone: UCHT1: cat. no. 555332; BD Biosciences) and PE-labeled anti-CD8 (clone HIT8a: cat. no. 555635; BD Biosciences) to characterize and categorize cytotoxic T cells; BV421-labeled anti-CD103 (clone: Ber-ACT8: cat. no. 563882; BD Biosciences) to identify T$_{RM}$ cells; and APC-labeled anti PD-1 (clone MIH4; BD Biosciences).

To assess T cell apoptosis, dead cells were stained with Fixable Viability Stain 780 (cat. no. 565388: BD Biosciences). Cells were subsequently permeabilized and fixed on ice for 20min using Fixation/Permeabilization Solution (BD Biosciences). The cells were then washed with Perm/Wash buffer (BD Biosciences) and stained with Alexa-Fluor 647-labeled anti-granzyme-B (clone: GB11: cat. no. 560212; BD Biosciences) at 4°C for 30min. Flow cytometry data were acquired on a BD LSRFortessa X-20 system (BD biosciences) equipped with FACSDiva software (BD Biosciences) and analyzed with FlowJo software, version 10 (Tree Star).

2.7 | Statistical analysis

All statistical analyses were performed using EZR,[17] which is R software with a modified version of R commander designed to add statistical functions frequently used in biostatistics. Fisher's exact probability test was used to compare categorical variables. Continuous variables were compared using the Mann–Whitney *U* test. Overall survival (OS) and relapse-free survival (RFS) curves were compared using the Kaplan–Meier method, and the significance of differences in survival was analyzed using the log-rank test. The date of surgery was set as the starting point for the measurement of OS. RFS was defined as the time between the date of surgery and recurrence. The Cox proportional hazard model was used for univariate and multivariate analyses of prognostic factors. The correlation between CD103 expression in metastatic LNs and primary lesions was examined using Spearman's rank correlation coefficient. Propensity score matching was performed to achieve balance of pStage II versus III/IV between CD103^{high} and CD103^{low}. Propensity scores were calculated using multivariate logistic regression models. Matching based on propensity scores was performed using a 1:1 nearest-neighbor algorism, with a caliper width of 0.2. *p*-values <0.05 were considered to indicate statistically significant differences.

3 | RESULTS

3.1 | Clinical importance of No. 106rec LNs

Of the 462 cases examined, 248 were pathologically positive for LN metastasis, of which 84 involved metastasis in No. 106rec LNs. Among the pN-positive cases, those with positive No. 106rec LNs also
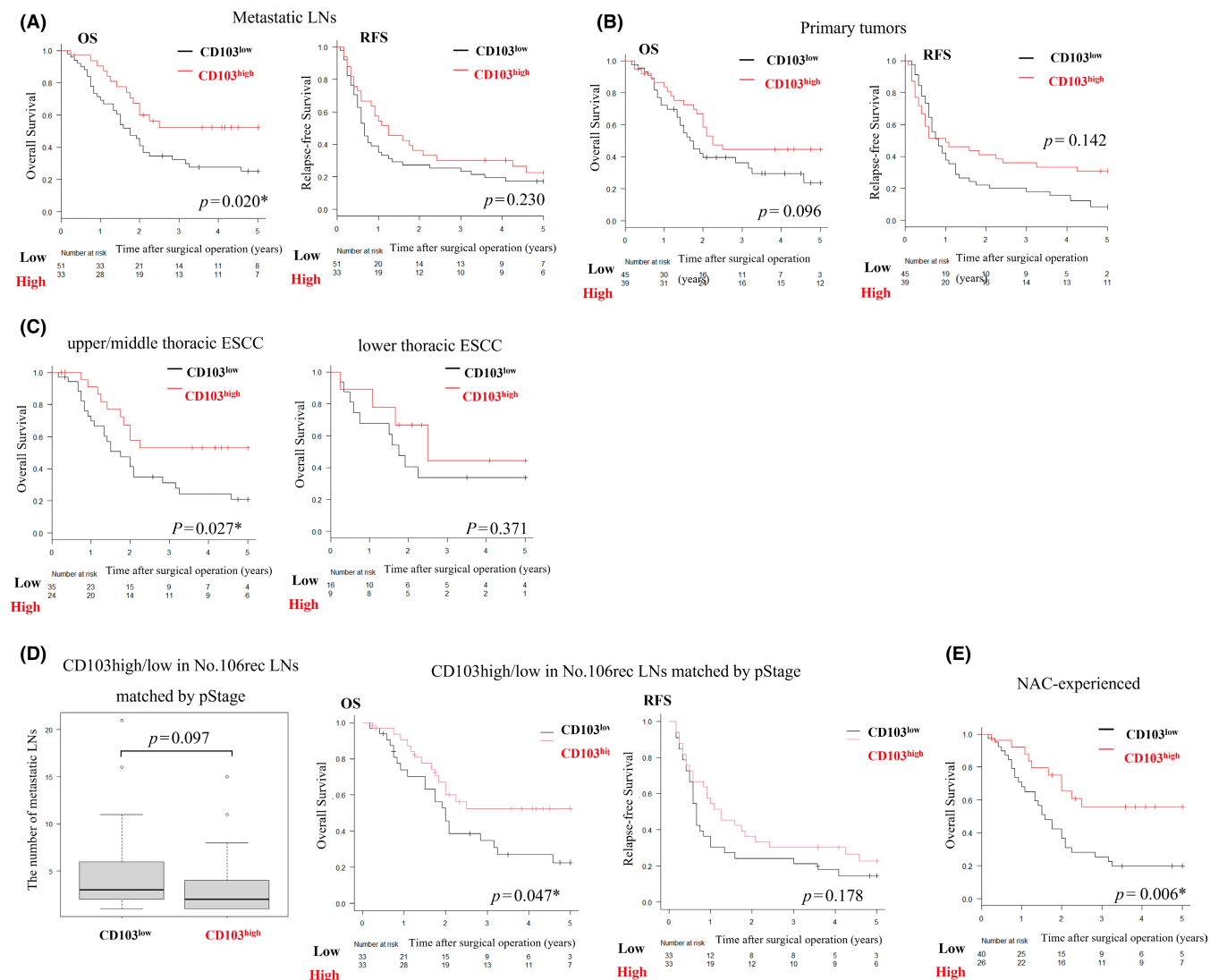
FIGURE 3 Prognostic effect of CD103$^+$ T cells as determined using Kaplan–Meier plots with the log-rank test and box plot. *$p < 0.05$, statistically significant. (A) Overall survival (OS) and RFS based on metastatic LNs. (B) OS and RFS based on primary tumors. (C) OS in Ut/Mt or Lt. (D) Comparison of the number of metastatic LNs, OS, and relapse-free survival (RFS) between CD103^{high} and CD103^{low} matched by pStage, and (E) OS in patients who received NAC.

had a significantly higher total number of LN metastases (Figure 1B). Prognosis was worse in patients with metastasis in No. 106rec LNs than in those without metastasis in these LNs, with 5-year survival rates of 44% and 70%, respectively (Figure 1C). This trend was the same whether the primary site was in the upper/middle or lower thoracic region (Figure 1D).

The effectiveness of No. 106rec LN dissection was evaluated based on the EI, which was calculated at 8.00, a relatively high value. These findings indicate that No. 106rec LNs are an important prognostic basis for thoracic esophageal cancer. Therefore, we focused on No. 106rec LNs to evaluate the immune microenvironment within LNs in esophageal cancer and its relationship to prognosis.

3.2 | Clinicopathological features of CD103+ cells in metastatic lymph nodes and primary lesions

Immunohistochemical analyses revealed few CD103$^+$ cells in non-metastatic LNs (Figure 2A). In contrast, a large number of CD103$^+$ cells were observed among LNs and primary tumors exhibiting pathological signs of metastasis, and these CD103$^+$ cells adhered to tumor cells as if infiltrating the metastatic tumor (Figure 2B,C,D). The number of CD103$^+$ cells infiltrating primary tumors showed a weak positive correlation with the number of CD103$^+$ cells in metastatic LNs ($r = 0.362$, $p = 0.0007$) (Figure 2E). We then classified the CD103$^+$ cells into two groups, CD103^{high}($n = 33$) and CD103^{low}($n = 51$), using ROC curves (The cut-off value; 28.8 cells per field) and examined the relationship

TABLE 2 pStage-matched cases (n = 66). Association between clinicopathological features and CD103 expression.

		CD103 + cells		
	n	Low (n = 33)	High (n = 33)	p-Value*
Age				
<60 year	49	22	27	0.26
>60 year	17	11	6	
Sex				
Female	5	2	3	1
Male	61	31	30	
Location				
Ut	19	10	9	0.732
Mt	32	17	15	
Lt	15	6	9	
Histological type				
Well	6	3	3	0.685
Moderate	37	19	18	
Poor	16	9	7	
Unknown	7	2	5	
Neoadjuvant chemotherapy				
+	50	24	26	0.775
−	16	9	7	
pT[a]				
T1/2	36	14	22	0.083
T3/4	30	19	11	
pN[a]				
N1	30	12	18	0.216
N2/3	36	21	15	
pStage[a]				
Stage II	23	8	9	1
Stage III/IV	49	25	24	
pN-JC[b]				
N1	26	11	15	0.634
N2	32	18	14	
N3	7	4	3	
N4	1	0	1	
Lymphatic invasion				
+	43	26	17	0.037*
−	23	7	16	
Venous invasion				
+	14	7	7	1
−	52	26	26	

*Fisher's exact probablity test; p < 0.05, statistically significant.
[a]TNM Classification of Esophageal squamous cell carcinoma, 8th ed.
[b]Japanese Classificasion of Esophageal Cancer, 11th ed.

with clinicopathological background (Table 1). No associations between most of the factors and CD103^{+} cell infiltration were observed. However, patients with advanced CD103^{+} cell infiltration exhibited less lymphatic invasion of the primary tumor and significantly fewer total LN metastases (Figure 2F).

3.3 | Intra-tumoral CD103+ cells in metastatic lymph nodes predict a good prognosis

We next investigated the prognostic effect of CD103^{+} cell infiltration in 84 patients with pathologic LN metastasis in No. 106rec LNs. Application of the Kaplan–Meyer method with the log-rank test showed that the CD103^{high} group had significantly longer OS (Figure 3A, p = 0.020). Regarding RFS, there was no difference between the groups (p = 0.230). CD103 expression in primary tumors was not associated with significant improvement in OS or RFS (Figure 3B). Among Ut/Mt ESCC cases, the CD103^{high} group had a better prognosis than the CD103^{low} group (Figure 3C, p = 0.0267). Moreover, to adjust the balance of pathological progression, we matched pStage based on propensity scores between CD103^{high} (n = 33) and CD103^{low} (n = 33) (Table 2). We compared the matched two groups for OS, RFS, and the total number of LN metastasis. Those results showed that there were no statistical differences in RFS and the number of LNs metastasis, but CD103^{high} prolonged OS significantly rather than CD103^{low} (Figure 3D).

Interestingly, among 65 patients who received NAC, the CD103^{high} group was associated with a much more favorable prognosis than the CD103^{low} group (Figure 3E, p = 0.006). The NAC regimen (FP:FGP:DCF) for the CD103^{high} group was 16:2:8; in contrast, that for the CD103^{low} group was 23:11:6 (p = 0.090). CD103^{+} cell infiltration within No. 106rec metastatic LNs was identified as an independent prognostic factor along with pathologic stage (Table 3).

3.4 | Phenotypes and activation markers of CD103^{+} T cells

We next examined whether CD103^{+} cells in the tissues function as effector cells. Simple immunohistochemical analysis using anti-CD8 and -CD103 antibodies suggested that CD103^{+} and CD8^{+} cells infiltrating tumors were identical, and double staining confirmed that many CD103^{+} cells directly infiltrating tumors in the LNs were also CD8^{+} (Figure 4A,B). Flow cytometry analysis indicated that 68% of CD8^{+} cells within metastatic LNs were also CD103^{+} (Figure 4C,D).

In contrast to the above results, a single-staining study of CD4^{+} cells showed little similarity between the distribution of CD103^{+} cells and tumor-infiltrating CD4^{+} cells (Figure 5A). CD103^{+} dendritic cells were also examined by double staining, but most CD103^{+} cells infiltrating tumors were CD11c^{−} (Figure 5B). In the immunohistochemistry of HLA-class I and II, tumor lesions of CD103^{low} had low expression on both HLA class I and II. In contrast, CD103^{high} expressed high HLA class I but expressed low HLA class II (Figure 5C).

The cytotoxic activity of CD103^{+} T cells was examined by double immunofluorescence staining of the intracellular cytokine granzyme B, which revealed that most of the CD103^{+} cells contained granzyme

TABLE 3 Univariate and multivariate analyses of prognostic factors in esophageal squamous cell carcinoma (ESCC) patients who received neoadjuvant chemotherapy.

| | 5-year overall survival | | | | | |
| | Univariate analysis | | | Multivariate analysis | | |
Variable	Hazard ratio	(95% CI)	*p*-Value*	Hazard ratio	(95% CI)	*p*-Value*
Age (<60 year/>60 year)	1.621	(0.715–3.677)	0.248			
Sex (Female/Male)	0.730	(0.323–1.654)	0.450			
Histological type (differentiated/ undiferentiated)	1.414	(0.753–2.655)	0.273			
Location (Ut, Mt/Lt)	0.835	(0.423–1.650)	0.604			
pT category (T1-2/T3-4)[a]	1.847	(0.965–3.536)	0.064			
pN category (N1/2–3)[a]	2.122	(1.068–4.214)	0.0317*			
pStage (II/III+IV)[a]	3.565	(1.258–10.10)	0.0167*	2.995	(1.047–8.568)	0.0408*
Lymphatic invasion (Ly−/Ly+)	2.322	(1.064–5.069))	0.0344*			
Venous invasion (V−/V+)	1.531	(0.773–3.031)	0.222			
CD103 (high/low) in primary lesions	0.612	(0.319–1.172)	0.138			
CD103 (high/low) in metastatic LNs	0.380	(0.185–0.783)	0.009*	0.442	(0.213–0.915)	0.0279*

*Cox proportional hazard mode; $p < 0.05$, statistically significant.

[a]TNM classification of esophageal squamous cell carcinoma, 8th ed.
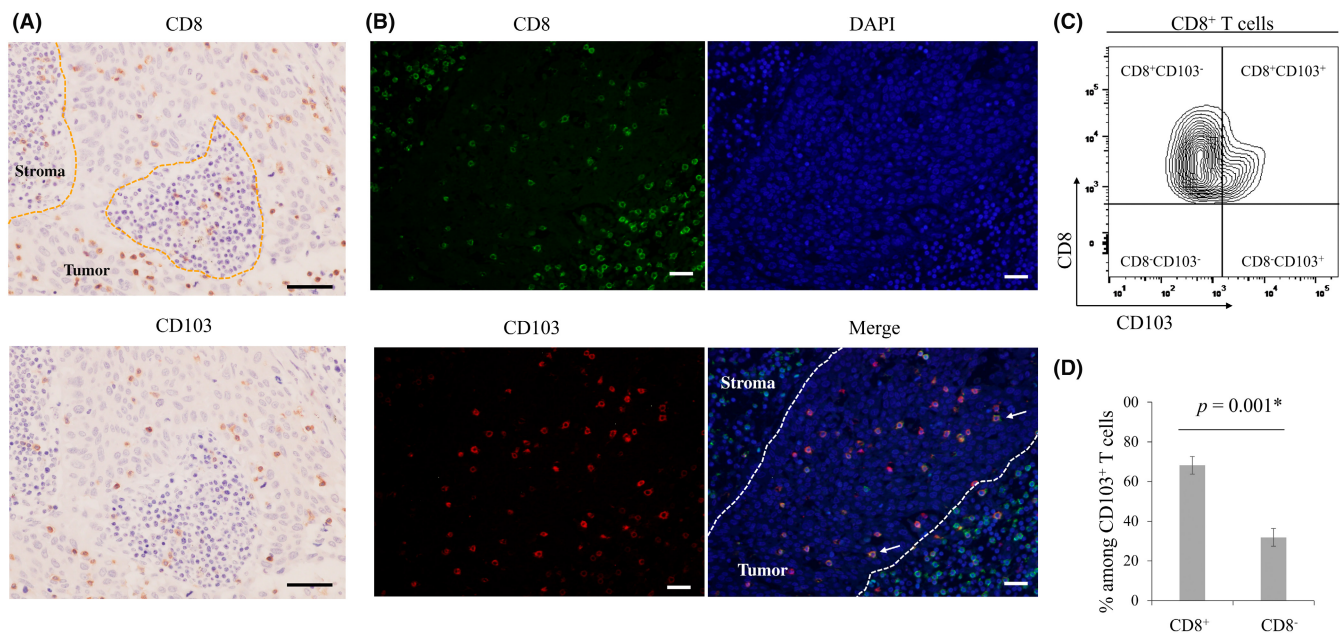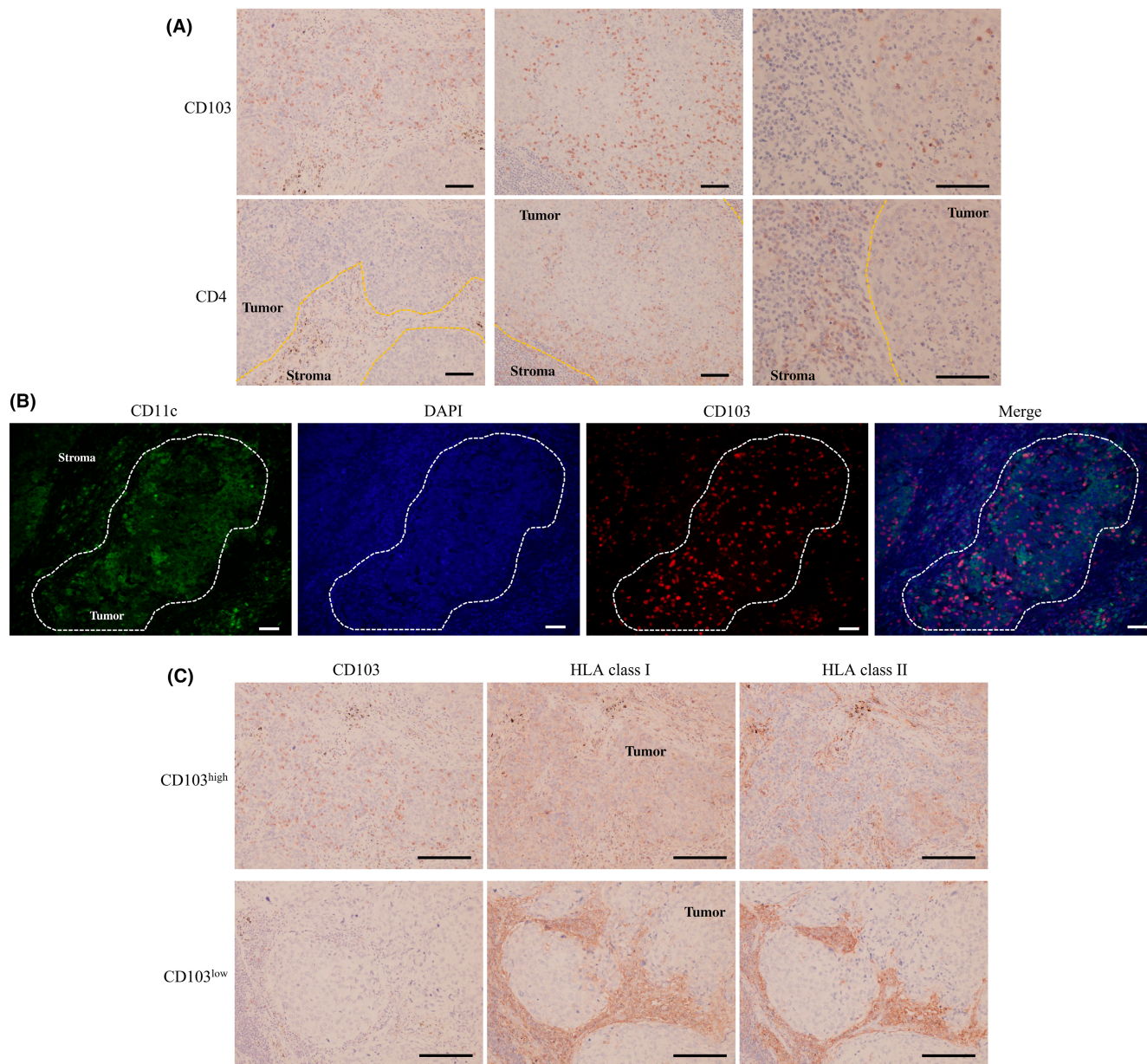

FIGURE 4 (A) Representative images of immunohistochemical analyses using anti-CD8 and anti-CD103 antibodies. Scale bar, 100 μm. (B) Representative images of immunofluorescence staining of CD8 (green), CD103 (red), and DAPI (blue) are shown. In tumoral lesions, most CD103+ cells also expressed CD8 (arrows). Scale bar, 100 μm. (C), (D) Flow cytometry analysis. (c) Representative contour plots of CD8+ T cells. (d) Bar graph shows the mean ± SE of the proportion of CD8+ and CD8− T cells among CD103+ T cells in metastatic lymph nodes (LNs) from eight esophageal cancer cases. CD8+CD103+ T cells accounted for 68.2% of CD103+ T cells. *$p < 0.05$, statistically significant.

B (Figure 6A). We also analyzed the production of cytokines by CD103+CD8+ T cells isolated from eight metastatic LNs. Flow cytometry analysis indicated that CD103+CD8+ T cells expressed higher levels of granzyme B than CD103−CD8+ T cells (Figure 6B). Approximately 90% of CD103+CD8+ cells contained granzyme B (Figure 6C). We also analyzed PD-1 expression of CD103+ cells within metastatic LNs. PD-1 among CD103+ T cells tended to express higher than CD103− cells, although there were no statistical significances (Figure 6D).

Finally, we examined the relationship between tumor E-cadherin expression and CD103 cell infiltration. CD103 cell infiltration was also observed in E-cadherin–negative cases, with no clear correlation (Figure 6E).
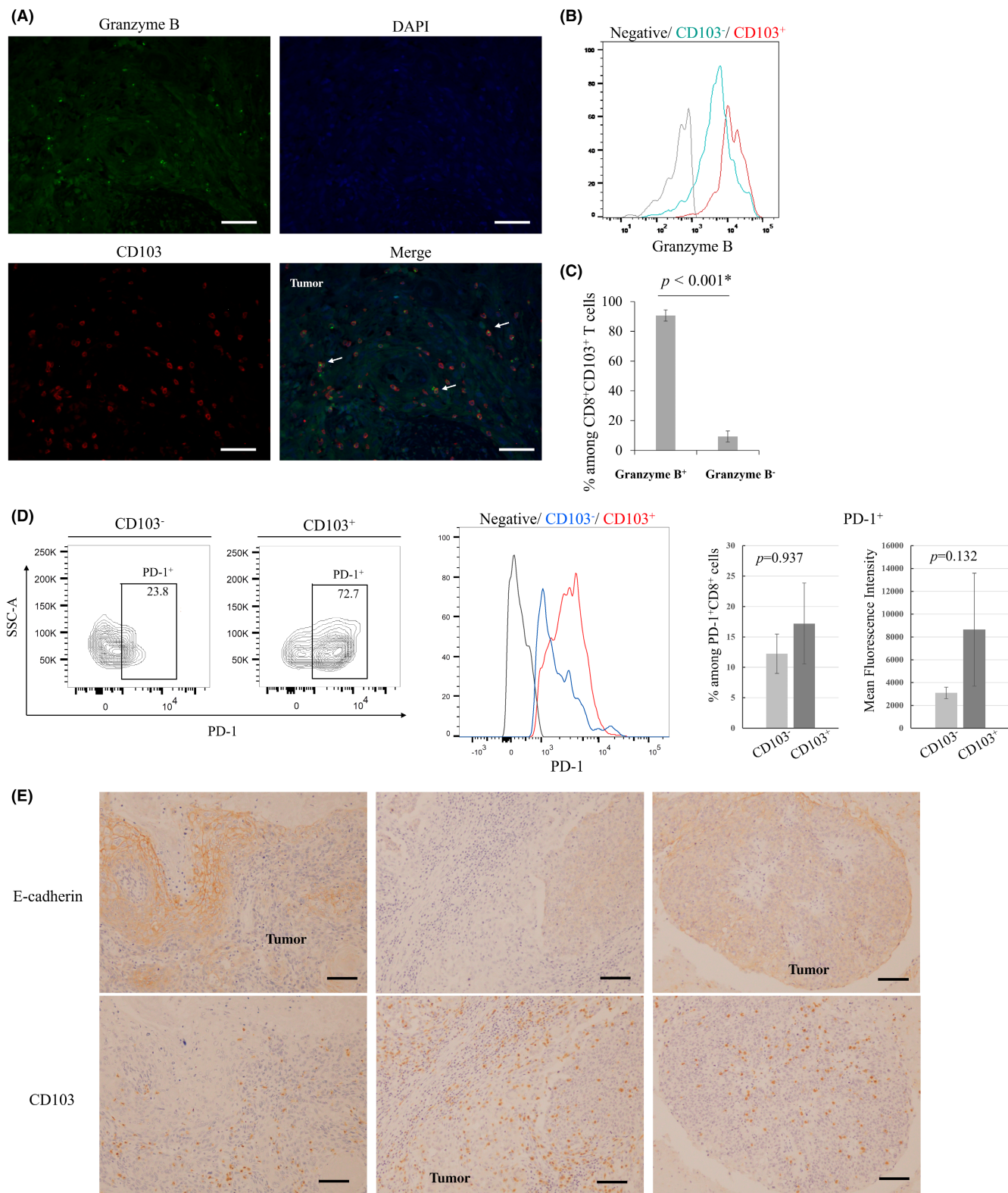
FIGURE 5 (A) Representative images of immunohistochemical analyses using anti-CD4 and anti-CD103 antibodies. Scale bar, 100 μm. (B) Representative images of immunofluorescence staining of CD11c (green), CD103 (red), and DAPI (blue). Scale bar, 100 μm. (C) Representative images of immunohistochemical analyses using anti-HLA class I/II and anti-CD103 antibodies. Scale bar, 100 μm.

4 | DISCUSSION

In this study, we found that CD103^{+} cells infiltrating LNs are also CD8^{+} effector cells in cases of metastasis to No. 106rec LNs, to which a high percentage of thoracic ESCC cells metastasize. We also found that many cases involving high infiltration of CD103^{+} cells have a good long-term prognosis. Our results thus suggest that CD103^{+} cells play an important role in the antitumor immune response in LNs.

Lymph nodes are considered important immune organs in the "cancer immune cycle," as they are involved in antigen presentation and induction of effector cells.[18] LNs around tumors may reflect the status of antitumor immunity to metastasis. Squamous

cell carcinoma of the thoracic esophagus is prone to extensive LN metastasis from the neck to the abdomen, and LN metastasis is the most important prognostic factor in such cancers. Among the thoracic LNs, No. 106rec LNs reportedly exhibit a high rate of metastasis, particularly in Ut/Mt ESCC, as the lymphatic flow tends to move upward into No. 106rec LNs.[19] The No. 106rec LNs are therefore considered sentinel LNs of thoracic ESCC.[4] Our data showed that the rate of metastasis to No. 106rec LNs and EI was high and that metastasis to several No. 106rec LNs was associated with a poorer prognosis. However, approximately 40% of patients with metastasis to No. 106rec LNs have a good long-term prognosis, suggesting these patients have an antitumor immune response in the No. 106rec LNs.

FIGURE 6 (A) Representative images of immunofluorescence double staining of CD103 (red), granzyme B (green), and DAPI (blue). CD103 cells that infiltrated tumoral lesions contained the intracellular cytokine granzyme B (arrows). Scale bar, 100 μm. (B), (C) Flow cytometry analysis of granzyme B in CD103$^+$CD8$^+$ T cells and CD103$^-$CD8$^+$ T cells. (B) Representative histogram. (C) Bar graph shows the mean ± SE of the proportion of granzyme B$^+$ and granzyme B$^-$ cells among CD8$^+$CD103$^+$ T cells. Granzyme B$^+$CD8$^+$CD103$^+$ T cells accounted for 90.7% of CD8$^+$CD103$^+$ T cells. (D) Flow cytometry analysis of PD-1 expression among CD103$^+$ cells and CD103$^-$ cells. Representative contour plots and histogram. Bar graphs show the mean ± SE of the proportion or the mean fluorescence intensity of PD-1 expression based on CD103 expression. (E) Representative images of immunohistochemical analyses using anti-CD103 and anti-E-cadherin antibodies. Scale bar, 100 μm.

Cytotoxic molecules produced by CD8$^+$CD103$^+$ T cells contribute to antitumor immunity and improve prognosis.[20] These CD8$^+$CD103$^+$ T cells are known as T$_{RM}$ cells and represent a subset of long-lived memory T cells that remain in the tissues.[21] We previously reported that gastric cancer patients with invasion of T$_{RM}$ cells into the primary tumor have a favorable prognosis.[12] In this study, we showed that approximately 70% of CD103$^+$ T cells also exhibit CD8 expression and that T$_{RM}$ cells produce higher levels of granzyme B than CD103$^-$CD8$^+$ T cells. Several studies showed CD8$^+$CD103$^+$ T cells account for 30–50% of CD103$^+$ T cells.[10,11] These results suggest that infiltrating T$_{RM}$ cells exert a strong cytotoxic function as effector T cells and that the antitumor immune response continues after the resection of tumors and regional LNs.

We also found that patients with invasion of CD103$^+$ cells who also received NAC had a better prognosis. We hypothesized that intra-tumoral CD103$^+$ T$_{RM}$ cells play a critical role in antitumor immunity after chemotherapy or immunogenic cell death. Our study showed no statistical significance in the NAC regimen between CD103^{high} and CD103^{low} but indicated the tendency of considerable DCF and little FGP. That result might suggest that docetaxel is likely to induce immunogenic cell death or that FGP receivers who commonly had renal dysfunction could not be adequately administered NAC. Therefore, invasion of CD103$^+$ cells might reflect the mounting of an antitumor immune response after NAC and could predict the effectiveness of immune checkpoint inhibitors (ICIs).

Where T$_{RM}$ cells reside and how they remain in those locations after surgical resection remain to be determined. Although patients with invasion of CD103$^+$ cells have a favorable prognosis, the tumors in which CD103$^+$ cells reside are resected during surgery. CD103$^+$ T$_{RM}$ cells are also associated with PD-1 expression and predict the effectiveness of ICI treatment,[12,22] as our result indicated a similar trend of higher PD-1 expression among CD103$^+$ cells than among CD103$^-$ cells. This might explain the presence of progenitor T$_{RM}$ cells in not-excised LNs or other organs. Several reports have suggested that circulating CD8$^+$ cells might adopt a T$_{RM}$ phenotype within the tumor and reside in the peripheral tissue after tumor resection.[23,24] Fang et al. (2021) reported that CD73 cells constitute a functionally distinct subset of memory T cells and resemble long-lived and polyfunctional memory T cells that could potentially develop into T$_{RM}$ cells.[25] Anadon et al. suggested that TCF1^{low} T$_{RM}$ cells could be regarded as stem-like T$_{RM}$ cells in ovarian cancer.[26] Today, multimodal approaches are used to treat ESCC, resulting in greater opportunities to use ICIs. These agents have changed the landscape of ESCC treatment and become key drugs. In this regard, further studies are needed to determine the origin and function of T$_{RM}$ cells.

We showed that whereas metastatic LNs harbor numerous CD103$^+$ cells, normal LNs harbor few of these cells. CD103, also known as integrin αE/β7, reportedly binds to the adherens junction protein E-cadherin in general and resides in peripheral tissues without secondary lymphoid organs.[27,28] E-cadherin plays an important role in mediating adhesion to adjacent keratinocytes, and a loss of E-cadherin leads to epithelial-mesenchymal transition and, ultimately, metastasis.[29] In this context, the prognostic effect of CD103 expression is reportedly associated with E-cadherin expression.[14] However, Webb et al. found no significant correlation between CD103 expression and E-cadherin staining intensity.[9] We also investigated this correlation by immunohistochemical analysis using several specimens, and we found that the presence of CD103 was not always equivalent to E-cadherin expression. Namely, the residency or infiltration of T$_{RM}$ cells might be induced by other molecules. For instance, T$_{RM}$ cells express various characteristic cell surface markers, including CD69, CD49a, and CD44.[13,27,28,30] These molecules also promote retention in peripheral tissues, including tumor sites.

Whether other phenotypes of CD103$^+$ cells are associated with improved survival must also be determined. Most CD103-expressing cells are CD8$^+$CD103$^+$ T$_{RM}$ cells, but some dendritic cells and regulatory T cells also express CD103.[31,32] We rarely detected CD103$^+$CD11c$^+$ cells in tumoral lesions. Djenidi et al. reported that CD103$^+$CD11c$^+$ cells represented only a small population of CD103$^+$ cells in human specimens[10]; in other words, CD103$^+$ dendritic cells in tumoral lesions were seldom associated with a favorable prognosis. CD103$^+$ cells can also exhibit a CD103$^+$CD4$^+$ phenotype. Although CD103$^+$ cells in tumors did not always match CD4$^+$ cells in our study, some previous studies showed that CD103$^+$CD4$^+$ T cells can exert an immunosuppressive effect and thus predict a poor prognosis.[32,33] By immunohistochemical analysis, we confirmed that the locations of CD103$^+$ cells differed from those of CD4$^+$ cells, and most of the CD103$^+$ cells were not regulatory T cells. Moreover, based on immunohistochemical analyses of HLA class I and II, it was evident that HLA class I was highly expressed in CD103^{high}, and HLA class II was barely expressed within tumor sites. These results might indicate that in tumor sites, CD103$^+$ cells were associated with HLA class I expression and not necessarily with HLA class II expression.

This study has several limitations. First, we only evaluated No. 106rec LN metastasis. Further studies will be needed to clarify the distribution of CD103$^+$ cells. Second, the number of samples subjected to flow cytometry analysis was low, and we did not examine many T$_{RM}$ cell subtypes and cytokines. Moreover, this study primarily employed immunohistochemistry and immunofluorescence staining; thus, we could not demonstrate the actual function of T$_{RM}$ cells. It would be helpful to investigate the development of T$_{RM}$ cells and the association between metastatic LNs and T$_{RM}$ cells in greater detail using other approaches.

In conclusion, we confirmed that CD103$^+$ T$_{RM}$ cells are present in metastatic LNs and associated with improved OS and controlled lymphatic invasion and metastasis. The results of this study enhance our understanding of the role of T$_{RM}$ cells in regional LNs and suggest the possibility of using their presence to predict prognosis or lymphatic metastasis in ESCC. A more complete understanding of the function and distribution of T$_{RM}$ cells could help clinicians identify regional LNs that should be resected in each case, thereby optimizing the extent of lymphadenectomy and minimizing surgery-related damage.

CONFLICT OF INTEREST STATEMENT

The authors have no conflict of interest.

ETHICS STATEMENT

Approval of the research protocol by an Institutional Reviewer Board/ Informed Consent: All experimental procedures after 2013 were approved by the Osaka City University Ethics Committee (approval No. 3138 and 4092), and all patients provided informed consent for collection and analysis of their specimens. In contrast, because the other experimental procedures up to 2013 were performed based on only all-inclusive consent, an opt-out form as for an observational study was used.

Registry and the Registration No. of the study/trial: N/A.

Animal Studies: N/A.

ORCID

Seiji Natsuki https://orcid.org/0000-0002-9714-5489
Takuya Mori https://orcid.org/0000-0002-0188-1116

REFERENCES

1. Arnold M, Soerjomataram I, Ferlay J, Forman D. Global incidence of oesophageal cancer by histological subtype in 2012. *Gut*. 2015;64(3):381-387.
2. Japan ES. Japanese classification of esophageal cancer, 11th edition: part I. *Esophagus*. 2017;14(1):1-36.
3. Tachimori Y, Ozawa S, Numasaki H, et al. Efficacy of lymph node dissection by node zones according to tumor location for esophageal squamous cell carcinoma. *Esophagus*. 2016;13:1-7.
4. Takeuchi H, Kitagawa Y. Sentinel node navigation surgery in esophageal cancer. *Ann Gastroenterol Surg*. 2019;3(1):7-13.
5. Han J, Khatwani N, Searles TG, Turk MJ, Angeles CV. Memory CD8(+) T cell responses to cancer. *Semin Immunol*. 2020;49:101435.
6. Stanton SE, Disis ML. Clinical significance of tumor-infiltrating lymphocytes in breast cancer. *J Immunother Cancer*. 2016;4:59.
7. Maibach F, Sadozai H, Seyed Jafari SM, Hunger RE, Schenk M. Tumor-infiltrating lymphocytes and their prognostic value in cutaneous melanoma. *Front Immunol*. 2020;11:2105.
8. Borsetto D, Tomasoni M, Payne K, et al. Prognostic significance of CD4+ and CD8+ tumor-infiltrating lymphocytes in head and neck squamous cell carcinoma: a meta-analysis. *Cancers (Basel)*. 2021;13(4):781.
9. Webb JR, Milne K, Watson P, Deleeuw RJ, Nelson BH. Tumor-infiltrating lymphocytes expressing the tissue resident memory marker CD103 are associated with increased survival in high-grade serous ovarian cancer. *Clin Cancer Res*. 2014;20(2):434-444.
10. Djenidi F, Adam J, Goubar A, et al. CD8+CD103+ tumor-infiltrating lymphocytes are tumor-specific tissue-resident memory T cells and a prognostic factor for survival in lung cancer patients. *J Immunol*. 2015;194(7):3475-3486.
11. Chu Y, Liao J, Li J, et al. CD103(+) tumor-infiltrating lymphocytes predict favorable prognosis in patients with esophageal squamous cell carcinoma. *J Cancer*. 2019;10(21):5234-5243.
12. Mori T, Tanaka H, Suzuki S, et al. Tertiary lymphoid structures show infiltration of effective tumor-resident T cells in gastric cancer. *Cancer Sci*. 2021;112(5):1746-1757.
13. Park SL, Gebhardt T, Mackay LK. Tissue-resident memory T cells in cancer Immunosurveillance. *Trends Immunol*. 2019;40(8):735-747.
14. Shields BD, Koss B, Taylor EM, et al. Loss of E-cadherin inhibits CD103 antitumor activity and reduces checkpoint blockade responsiveness in melanoma. *Cancer Res*. 2019;79(6):1113-1123.
15. Brierley JD, Gospodarowicz MK, Wittekind C. *TNM Classification of Malignant Tumours*. 8th ed. Wiley Blackwell; 2017.
16. Udagawa H, Ueno M, Shinohara H, et al. The importance of grouping of lymph node stations and rationale of three-field lymphoadenectomy for thoracic esophageal cancer. *J Surg Oncol*. 2012;106(6):742-747.
17. Kanda Y. Investigation of the freely available easy-to-use software 'EZR' for medical statistics. *Bone Marrow Transplant*. 2013;48(3):452-458.
18. Chen DS, Mellman I. Oncology meets immunology: the cancer-immunity cycle. *Immunity*. 2013;39(1):1-10.
19. Kato H, Iizuka T, Terui S. The lymphatics of the esophagus, studied with the aid of lymphoscintigraphy. *Jpn J Gastroenterol Surg*. 1985;18(3):599-606.
20. Yenyuwadee S, Sanchez-Trincado Lopez JL, Shah R, Rosato PC, Boussiotis VA. The evolving role of tissue-resident memory T cells in infections and cancer. Science. *Advances*. 2022;8(33):eabo5871.
21. Mackay LK, Stock AT, Ma JZ, et al. Long-lived epithelial immunity by tissue-resident memory T (TRM) cells in the absence of persisting local antigen presentation. *Proc Natl Acad Sci USA*. 2012;109(18):7037-7042.
22. Han L, Gao QL, Zhou XM, et al. Characterization of CD103(+) CD8(+) tissue-resident T cells in esophageal squamous cell carcinoma: may be tumor reactive and resurrected by anti-PD-1 blockade. *Cancer Immunol Immunother*. 2020;69(8):1493-1504.
23. Enamorado M, Iborra S, Priego E, et al. Enhanced anti-tumour immunity requires the interplay between resident and circulating memory CD8+ T cells. *Nat Commun*. 2017;8(1):16073.
24. Sun H, Sun C, Xiao W, Sun R. Tissue-resident lymphocytes: from adaptive to innate immunity. *Cell Mol Immunol*. 2019;16(3):205-215.
25. Fang F, Cao W, Zhu W, et al. The cell-surface 5′-nucleotidase CD73 defines a functional T memory cell subset that declines with age. *Cell Rep*. 2021;37(6):109981.
26. Anadon CM, Yu X, Hänggi K, et al. Ovarian cancer immunogenicity is governed by a narrow subset of progenitor tissue-resident memory T cells. *Cancer Cell*. 2022;40(5):545-557.e13.
27. Amsen D, van Gisbergen K, Hombrink P, van Lier RAW. Tissue-resident memory T cells at the center of immunity to solid tumors. *Nat Immunol*. 2018;19(6):538-546.
28. Mami-Chouaib F, Blanc C, Corgnac S, et al. Resident memory T cells, critical components in tumor immunology. *J Immunother Cancer*. 2018;6(1):87.

29. van Roy F. Beyond E-cadherin: roles of other cadherin superfamily members in cancer. *Nat Rev Cancer.* 2014;14(2):121-134.

30. Topham DJ, Reilly EC. Tissue-resident memory CD8(+) T cells: from phenotype to function. *Front Immunol.* 2018;9:515.

31. Maier B, Leader AM, Chen ST, et al. A conserved dendritic-cell regulatory program limits antitumour immunity. *Nature.* 2020;580(7802):257-262.

32. Ichikawa T, Hirahara K, Kokubo K, et al. CD103(hi) T(reg) cells constrain lung fibrosis induced by CD103(lo) tissue-resident pathogenic CD4 T cells. *Nat Immunol.* 2019;20(11):1469-1480.

33. Gu Y, Chen Y, Jin K, et al. Intratumoral CD103(+)CD4(+) T cell infiltration defines immunoevasive contexture and poor clinical outcomes in gastric cancer patients. *Onco Targets Ther.* 2020;9(1):1844402.

SUPPORTING INFORMATION

Additional supporting information can be found online in the Supporting Information section at the end of this article.